Antiviral Research 92 (2011) 461–469

Contents lists available at SciVerse ScienceDirect

Antiviral Research

journal homepage: www.elsevier.com/locate/antiviral

Novel plant-derived recombinant human interferons with broad spectrum antiviral activity

Jeffrey W. Koehler [a], Lesley C. Dupuy [a], Aura R. Garrison [a], Brett F. Beitzel [a], Michelle J. Richards [a], Daniel R. Ripoll [b], Anders Wallqvist [b], Shia-Yen Teh [c], Andrew A. Vaewhongs [d], Fakhrieh S. Vojdani [d], Hal S. Padgett [d], Connie S. Schmaljohn [a,*]

[a] U.S. Army Medical Research Institute of Infectious Diseases, Virology Division, Fort Detrick, MD 21702, USA
[b] U.S. Army Medical Research and Materiel Command, Telemedicine and Advanced Technology Research Center, Biotechnology HPC Software Applications Institute, Fort Detrick, MD 21702, USA
[c] University of California-Irvine, Irvine, CA 92697, USA
[d] Novici Biotech LLC, Vacaville, CA 95688, USA

ARTICLE INFO

Article history:
Received 12 August 2011
Revised 27 September 2011
Accepted 7 October 2011
Available online 14 October 2011

Keywords:
Type I interferons
Ebola virus
Rift Valley fever virus
Venezuelan equine encephalitis virus
Monkeypox virus

ABSTRACT

Type I interferons (IFNs) are potent mediators of the innate immune response to viral infection. IFNs released from infected cells bind to a receptor (IFNAR) on neighboring cells, triggering signaling cascades that limit further infection. Subtle variations in amino acids can alter IFNAR binding and signaling outcomes. We used a new gene crossbreeding method to generate hybrid, type I human IFNs with enhanced antiviral activity against four dissimilar, highly pathogenic viruses. Approximately 1400 novel IFN genes were expressed in plants, and the resultant IFN proteins were screened for antiviral activity. Comparing the gene sequences of a final set of 12 potent IFNs to those of parent genes revealed strong selection pressures at numerous amino acids. Using three-dimensional models based on a recently solved experimental structure of IFN bound to IFNAR, we show that many but not all of the amino acids that were highly selected for are predicted to improve receptor binding.

Published by Elsevier B.V.

1. Introduction

Type I interferons (IFNs), including IFN-α and IFN-β, play critical roles in the antiviral innate immune response and are induced in response to unique components of viral infection such as double-stranded RNA. After secretion from infected cells, IFN binds to a receptor (IFNAR) on nearby cells, initiating signaling cascades that enhance cellular resistance to viral infection [reviewed in (Platanias, 2005; Samuel, 2001)]. IFN-α/β are the best studied of the type I human IFNs, and IFN-α therapy has been successful in treating viral infections in people, most notably hepatitis C (Carreno et al., 1987; Fried et al., 2002). Advances in IFN-α therapy include: (1) the addition of a branched 40 kDa polyethylene glycol molecule (pegylation) to synthetic IFN-α, which enhances the effective half-life of the IFN when compared to its native form (Glue et al., 2000); and, (2) use of a synthetic IFN-α (IFN-alfacon-1), which contains the most frequently observed amino acids among several natural IFN-α subtypes (Ozes et al., 1992). These synthetic IFNs are currently manufactured using bacterial expression methods.

Most viruses, including highly pathogenic viruses such as Venezuelan equine encephalitis (VEEV), Rift Valley fever (RVFV), Ebola (EBOV), and monkeypox (MPXV) viruses, have developed methods to counteract the antiviral effects of IFNs (Bouloy et al., 2001; Fernandez de Marco Mdel et al., 2009; Mateo et al., 2010; Simmons et al., 2009; Weaver and Isaacs, 2008; Yin et al., 2009). Treatment options for these viruses are limited and can include ribavirin (Jahrling et al., 1980), small interfering RNAs (Geisbert et al., 2010), and double-stranded RNA activated caspase oligomerizers (Rider et al., 2011). Potent IFNs, especially those that could overcome the viral IFN antagonistic mechanisms, would provide additional broad spectrum options for prophylaxis and therapy.

Here we report studies aimed at generating novel type I IFNs with broad spectrum activity against VEEV, RVFV, EBOV, and MPXV. We used a new gene crossbreeding method termed Genetic ReAssortment by MisMatch Resolution (GRAMMR™), which combines a mismatch endonuclease with a proofreading polymerase and ligase to resolve unpaired bases in heteroduplexes, which are produced by melting and annealing genes within an expression

Abbreviations: IFNs, interferons; IFNAR, interferon-α receptor; VEEV, Venezuelan equine encephalitis virus; RVFV, Rift Valley fever virus; EBOV, Ebola virus; MPXV, monkeypox virus; GRAMMR™, Genetic Reassortment by MisMatch Resolution; BSA, bovine serum albumin; GFP, green fluorescent protein; PSPP, protein structure prediction pipeline; PDB, Protein Data Bank.

* Corresponding author. Tel.: +1 301 619 4103; fax: +1 301 619 2439.
E-mail address: connie.schmaljohn@amedd.army.mil (C.S. Schmaljohn).

0166-3542/$ - see front matter Published by Elsevier B.V.
doi:10.1016/j.antiviral.2011.10.008

vector. We chose plants rather than bacteria to express the hybrid IFNs because of advantages they offer such as ease of use, high yield of expression products, ability to produce secreted proteins, and mechanisms for oxidative cross-linking of cysteines for proper folding (Giritch et al., 2006; Ma et al., 2003). Also, hundreds of plants can be individually inoculated in parallel, making it possible to rapidly produce and evaluate numerous potential candidate expression products. Our results demonstrate that it is possible to create new human IFNs with improved activity against very diverse viruses and that the improvements can be partially traced to subtle amino acid changes that are predicted to influence their binding to IFNAR.

2. Materials and methods

2.1. Production of the hybrid IFN library

IFN-α2a reference standard (Gxa01-901-535) was obtained from the NIAID Reference Reagent Repository operated by Braton Biotech, Inc. in Gaithersburg MD. Pharmaceutical grade consensus IFN-α (IFN-alfacon-1) reference standard (Infergen; Valeant) was obtained by prescription from a pharmacy. IFN-α1, -α2a, -α4, -α5, -α8, -α10, -α21, IFN-β, IFN-ε, IFN-κ, and IFN-ω genes and genes for the controls IFN-α2a, green fluorescent protein (GFP), and alfacon-1 were codon-optimized for plant expression (see Fig. 4 for IFN amino acid sequences) and inserted into the tobamovirus vector pLSBC-DN15 (O'Keefe et al., 2009) containing a N-terminal extensin secretory signal peptide from *Nicotiana plumbaginifolia* (De Loose et al., 1991) and a C-terminal 6xHis tag with the KDEL endoplasmic retention sequence (Munro and Pelham, 1987). Hybrid libraries were generated using GRAMMR™ (US Patents; 7056,740, 7217,514, and 7833,759). Plasmid heteroduplexes were generated by linearizing the pLSBC-DN15-interferon genes with *Stu*I or *Sma*I, heating to 95 °C to dissociate the DNA strands, and cooling to allow strands to anneal. Heteroduplex DNAs were incubated with *Res*I, a mismatch endonuclease from *Selaginella lepidophylla* (US Patents; 7056,740, 7217,514, and 7833,759), T4 DNA polymerase, and *Escherichia coli* DNA ligase. After one h at 25 °C, DH5-α cells (Invitrogen, Carlsbad, CA) were transformed to isolate individual hybrid plasmids. Infectious viral RNA transcripts from these plasmids were generated using the mMessage mMachine kit (Ambion, Austin, TX).

Four-week old *Nicotiana benthamiana* plants were inoculated with infectious RNA by manual abrasion with diatomaceous earth. Approximately 2 g of plant tissue were homogenized [150 mM Tris–HCl buffer (pH 8.2), 0.5 M NaCl, 15 mM imidazole, 2 mM PMSF, 0.15% sodium metabisulfite] 5–7 days post-inoculation. Clarified homogenates were purified using nickel-conjugated agarose beads (Qiagen, Valencia, CA) using wash buffer [50 mM Tri–HCl (pH 8.2), 0.5 M NaCl, 10 mM imidazole, 0.01% Na metabisulfite, 0.2 mM PMSF] and elution buffer [0.4 M imidazole-0.1 M Tris–HCl (pH 8.2) with 0.2 mg/ml bovine serum albumin (BSA)]. Expressed protein was quantified by densitometry of Coomassie blue-stained SDS–PAGE gels using standards of plant-produced, untagged IFN-α2a protein. The concentration of each protein was adjusted to 75 ng/ml in phosphate-buffered saline (PBS), pH 7.4, containing 1 mg/ml BSA, and IFN concentrations were determined again using densitometry. IFNs and GFP were diluted 10-fold in RPMI 1640 supplemented with 2 mM L-glutamine, 10 mM HEPES, 1 mM sodium pyruvate, 4.5 g/L glucose, 1.5 g/L sodium bicarbonate, and 10% FBS for further studies. Low-yielding clones were omitted from subsequent rounds of GRAMMR.

2.2. Viruses and cells

Luciferase-tagged RVFV rMP12-rluc (Ikegami et al., 2006) virus was kindly provided by Dr. Shinji Makino of the University of Texas Medical Branch at Galveston. The GFP-tagged Zaire ebolavirus, EboZ-eGFP (Palacios et al., 2007), was kindly provided by Dr. Jonathan Towner, Centers for Disease Control and Prevention. The MPXV-GFP virus was produced as previously described (Goff et al., 2011). To generate luciferase-tagged VEEV, a *Not*I-flanked firefly luciferase expression cassette was cloned into a plasmid containing VEEV, strain Trinidad donkey, nsP3 having *Not*I restriction sites inserted at random locations (Beitzel et al., 2010). The nsP3-luciferase fusions were excised and cloned into a full-length genomic clone of VEEV, strain Trinidad donkey. Infectious RNA was transcribed and transfected into BHK cells to generate replication-competent VEEV containing the luciferase expression cassette. Luciferase activity was assessed 24 h post-infection on Vero cells using the Steady-Glo luciferase assay system (Promega, Madison, WI). Plaque-picked virus, which contained a fusion at nucleotide 5431 (GenBank Accession No. L01442), maintained cytopathic effects and luciferase activity, was selected for this study.

Vero and Vero 76 cells were used for the antiviral screening assays. Cells were maintained in either DMEM supplemented with 10% FBS (for RVFV and VEEV) or MegaVir (Hyclone, Logan, UT; for EBOV and MPXV).

2.3. Antiviral and antiproliferative assays

Confluent cells in 96-well luminometer plates were treated with IFN (approximately 60,000 to 1 pg/ml) for 24 h before being infected with a signal-optimized amount of reporter virus. The luciferase-tagged VEEV and RVFV assays were read 18 h post infection using the Steady-Glo (VEEV) or *Renilla* (RVFV) luciferase assay systems (Promega, Madison, WI) according to the manufacturer's instructions. For VEEV, Steady-Glo reagent containing both lysis buffer and luciferase substrate was added to the wells, and luciferase activity was measured. For RVFV, the media was removed from the cell monolayers, and *Renilla* lysis buffer was added to release the luciferase enzyme. Luciferase substrate was added, and luminescence was measured. The GFP-tagged viruses, MPXV and EBOV, were assayed for fluorescence 48 h after infection. Daudi cell-proliferation assays were conducted as previously described (Nederman et al., 1990). For these assays luciferase activity was recorded as relative light units (RLU), and for the GFP-based assays, fluorescence activity was recorded as relative fluorescence units (RFU). Initially, IFNs from early rounds of screening were evaluated for antiviral activity with EBOV, and promising hybrid IFNs were included in the additional rounds of GRAMMR. For subsequent evaluations, all four reporter viruses were included in the antiviral screenings.

2.4. Protein modeling

The Protein Structure Prediction Pipeline (PSPP) (Lee et al., 2009), initially developed for domain boundary detection, sequence homology search, fold recognition, homology modeling, de novo design, and model evaluation, was used to generate three-dimensional models for the high-potency IFNs from sequence. The PSPP uses the program NEST (Petrey et al., 2003) for generating homology models. Two data inputs were used to produce these models: (a) template files from the experimentally determined structures of IFN-α2a (Klaus et al., 1997) and IFN-α2 bound to an IFN-αβ receptor (Nudelman et al., 2010) [Protein Data Bank (PDB) (Berman et al., 2000)]; and (b) pair-wise alignments between each of the target IFN sequences and that of the template structures. Models based on different templates were built to assess the variability of unique parts of the structure, particularly those involving regions of the IFN molecules that were expected to be in contact with the receptor. Analysis of the final structures

was performed with the help of PyMOL Molecular Graphics System (pymol.org) and DS-Modeling (Accelrys, San Diego, CA).

2.5. Statistical analysis

Data were analyzed using GraphPad Prism 5 (GraphPad Software, La Jolla, CA) using a nonlinear, variable slope regression analysis. Each hybrid IFN was compared to the control IFN-α2a-His using the extra sum-of-squares F test to determine if there was a significant difference between the IFN concentration required to decrease viral or Daudi cell replication by 50 (IC_{50}) or 90 (IC_{90}) percent. Statistical significance cutoff was $P < 0.05$.

3. Results

3.1. GRAMMR production of hybrid IFN genes and expression in plants

Parent IFN genes were cloned into a tobamovirus-based plant expression vector, and hybrid gene libraries were generated using GRAMMR. *N. benthamiana* plants were inoculated with infectious RNAs transcribed from the hybrid genes, and His-tagged IFNs were purified, resolved, and quantified by SDS–PAGE (Fig. 1). We generated an initial library with IFN-α1, -α2a, -α4, -α5, -α8, -α10, and -α21 parental subtype genes, which share nucleotide identities from 88% to 97%. This library was screened for antiviral activity against EBOV. One hybrid IFN comprised of IFN-α8 and four contiguous amino acids from IFN-α5 (termed IFN-5/8 Hyb) had strong antiviral activity and high protein yields in plants (data not shown). This IFN was included in subsequent rounds of GRAMMR. Libraries were also produced by pairings of IFN-α genes with IFN-β, -ε, -κ, or -ω genes. The IFN-α subtype genes shared 77–79% identity with IFN-ω and 55–63% identity with the IFN-β, -ε, and -κ genes. Overall, a single-round of GRAMMR resulted in an average of 9–13 crossovers/kb for the IFN-α/IFN-α subtype libraries; IFN-α genes combined pair-wise with IFN-β, -ε, -κ, or -ω genes contained an average of about 3.5 crossovers/kb. Approximately 1400 hybrids were produced with the IFN-α parental subtypes while only 180 of the ∼2000 IFN-α/ IFN-β,-ε,-κ hybrid IFNs produced enough protein for further studies. A sampling of the IFN library was analyzed by mass spectrometry (MALDI-TOF) to verify protein size and folding (data not shown).

3.2. Selection of hybrid IFNs with increased antiviral activity

To establish a baseline for later comparisons, we pretreated cells with our plant-derived IFN-α2a-His or with the NIH reference standard IFN-α2a and then infected the cells with RVFV or VEEV reporter viruses. Viral replication (luciferase activity) measured 18 h post-infection showed the plant- and bacteria-derived IFN-α2a proteins have similar inhibition kinetics; thus, neither plant expression nor the His-tag appeared to be deleterious to the antiviral effects of the IFN (Fig. 2, A and B). We also compared the antiviral activities of pharmaceutical-grade IFN-alfacon-1 (Infergen), IFN-α2a-His, and plant-derived IFN-alfacon-1-His. Based on calculated inhibitory concentrations (IC_{50} and IC_{90} values), both the plant-derived and bacteria-derived IFN-alfacon proteins inhibited RVFV and VEEV better than IFN-α2a-His. IFN-alfacon-1-His (plant) and Infergen inhibited similarly (Fig. 2C, D, and Supplemental Table 1).

After several rounds of GRAMMR, the antiviral activities of the hybrid IFNs were assessed against all four reporter viruses (RVFV, VEEV, EBOV, and MPXV). The plant-derived IFN-alfacon-1-His

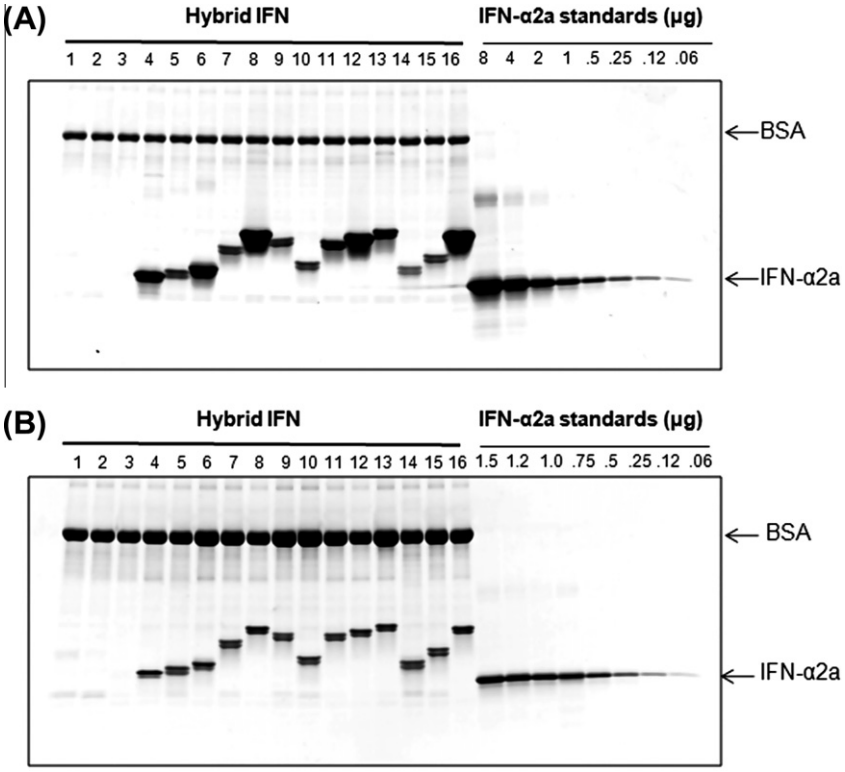

Fig. 1. Comparison of hybrid IFN protein yields from *N. benthamiana* plant homogenates. His-tagged, hybrid IFN proteins were purified from plant homogenates by binding to Ni-conjugated agarose beads. A sample of each purified hybrid IFN was analyzed by SDS–PAGE and staining with Coomassie blue, then quantified by densitometry as compared to standards of plant-produced, untagged IFN-α2a. (A) Relative yields of IFNs are shown before normalization. Lanes 1–3 are samples that were rejected due to low yields. (B) Samples were normalized (except for those in lanes 1–3) and quantified using a narrower range of standards for comparison. The top arrow indicates BSA, which was included in the purification buffer to stabilize the IFN proteins. The bottom arrow indicates the IFN-α2a standard.

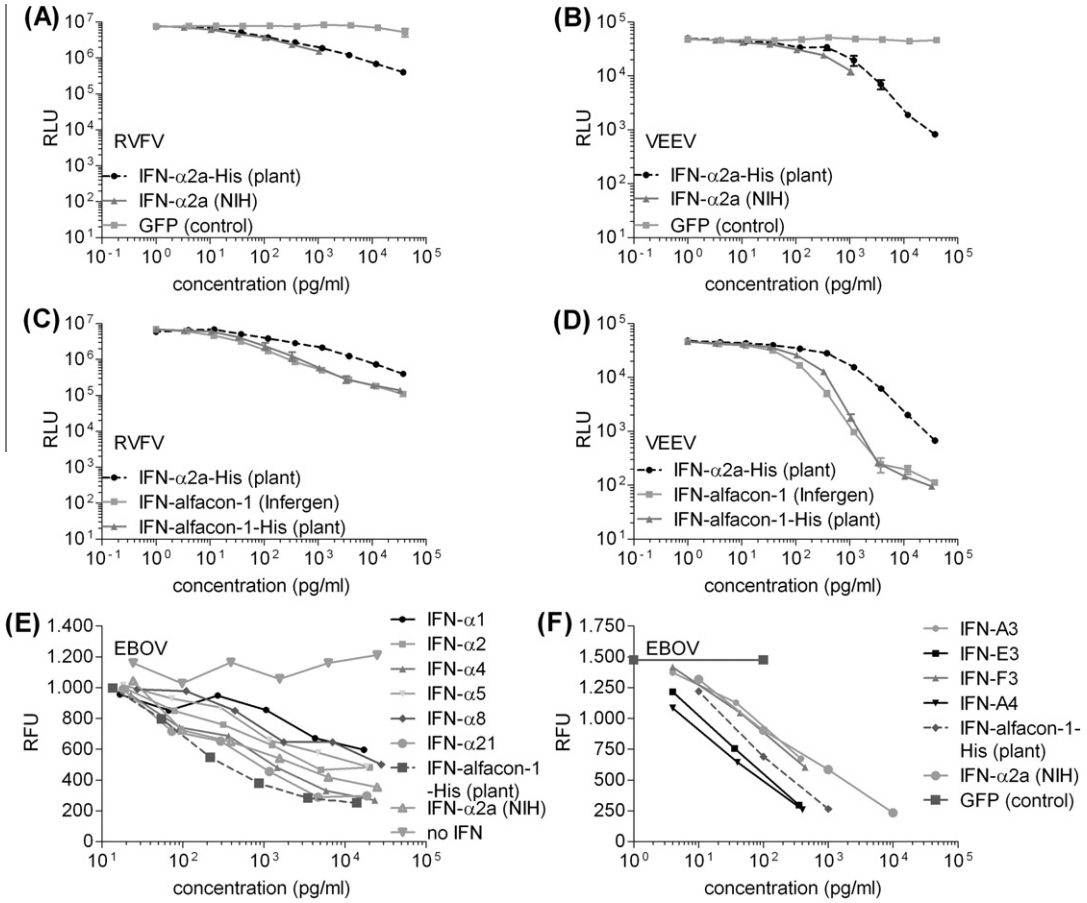

Fig. 2. Antiviral activities and down selection of plant derived IFNs. (A and B) Inhibition of the RVFV and VEEV luciferase reporter viruses were compared for IFN-α2a-His (plant) and the NIH standard IFN-α2a (NIH) or (C and D) pharmaceutical-grade IFN-alfacon-1 (Infergen) and the plant-expressed IFN-alfacon-1-His (plant). (E and F) Inhibition of the EBOV-GFP reporter virus by parental IFN, IFN alfacon-1-His (plant), IFN-α2a (NIH), and hybrid IFNs generated in early rounds of GRAMMR was compared. Cells were incubated with IFN 24 h prior to infection, and relative light units (RLU) or relative fluorescence units (RFU) were measured after 18 h or 48 h, respectively. The GFP control was comprised of a 6xHis-KDEL tagged GFP gene, expressed in plants, and is intended to demonstrate that these modifications and plant expression by themselves do not interfere with viral replication. Each concentration was run in duplicate (A–E), and error bars indicate standard deviation. Tests for significance are shown in Supplemental Table 1.

showed stronger antiviral activity than any of the parental IFNs (e.g., Fig. 2E, with EBOV). Most of the IFN-α/IFN-α and IFN-α/IFN-ω hybrids were active against one or more of the viruses, and several showed stronger activity than IFN-alfacon-His (e.g., Fig. 2F, IFN-E3 and IFN-A4 with EBOV). In contrast, about one-third of the IFN-α/IFN-β, IFN-α/IFN-ε, or IFN-α/IFN-κ hybrids showed little or no antiviral activity, indicating that dramatic shifts in protein sequence/structure might not be tolerated. Seventy-five candidates showing broad spectrum and/or enhanced inhibition compared to controls were selected for confirmatory screening resulting in the identification of 12 potent IFNs (FINAL-12) including 11 hybrid IFNs that had undergone several rounds of GRAMMR as well as IFN-5/8 Hyb (data not shown).

The FINAL-12 IFNs were arrayed in triplicate over a wide range of concentrations, and antiviral properties re-assessed. IFN-α2a-His was used for comparison because it showed more consistent activity than IFN-alfacon-1 in our assays. To control for the possibility that the antiviral activity measured was related to reduction in cell proliferation rather than to a direct effect on the virus, Daudi inhibition assays were performed using an Epstein–Barr virus-transformed human B-cell line that is highly sensitive to IFN-α (Nederman et al., 1990). None of the hybrid IFNs showed significantly greater anti-proliferative activity compared to IFN-α2a for both IC_{50} and IC_{90} values (Supplemental Table 2). In contrast, most of the FINAL-12 hybrid IFNs continued to demonstrate significantly enhanced antiviral activity against RVFV and VEEV as compared to the plant-derived IFN-α2a-His control (Supplemental Table 3). Similar statistical analyses were not possible for EBOV and MPXV because of the poor activity of the control IFN-α2a against these viruses. Nevertheless, we observed that many of the hybrid IFNs did inhibit viral replication, especially for EBOV, as indicated by both leftward and downward shifts in their dose–response curves (e.g., Fig. 3, IFN-B4 and IFN-H3).

3.3. Sequence comparisons and structural modeling

Amino acid sequences for the parental IFNs and the hybrid IFNs were aligned, specifically looking for changes in amino acids known to be important for binding to IFNAR-1 and IFNAR-2 (Piehler and Schreiber, 1999; Slutzki et al., 2006; Uze et al., 2007), the two subunits of IFNAR (Fig. 4). In general, IFN binds initially to IFNAR-2 with high affinity followed by lower affinity binding to IFNAR-1, initiating signaling cascades [reviewed in (Uze et al., 2007)]. Previous studies suggest that potent IFNs have more positively-charged C-terminal tail residues, which interact with a negatively charged region of IFNAR-2 (Slutzki et al., 2006). Similarly, most of our hybrid IFNs have positive tails with five of them sharing a +4 charge (KRLRRKE) not observed in any of the parents and six others having a net +3 charge tail.

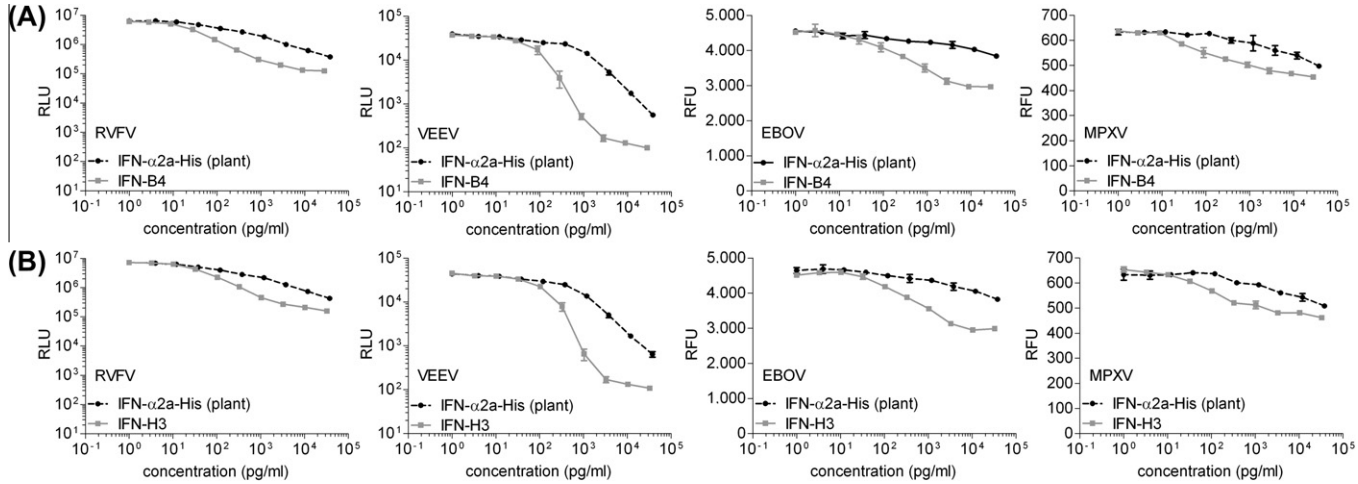

Fig. 3. Inhibitory activities of two examples of hybrid IFNs. Cells were incubated with hybrid IFN-B4 (A), IFN-H3 (B), or IFN-α2a-His for 24 h before infection with RVFV- or VEEV- luciferase reporter viruses, or EBOV- or MPXV-GFP reporter viruses. Relative light units (RLU) or relative fluorescence units (RFU) were measured after 18 h or 48 h, respectively. Each concentration was run in triplicate, and error bars indicate standard deviation. Tests for significance are shown in Supplemental Table 3.

To explore the influences of these charges on IFNAR binding, we used a recent experimental structure of IFN-α2 in complex with IFNAR-2 (Nudelman et al., 2010) (PDB code:2KZ1) to model IFN-H3, which has a +4 charged tail. Three residue-residue interactions involving salt bridge formation are predicted: IFN-H3 residues R163, R164, and K165 with IFNAR-2 residues D70, E134, and E133, respectively (Fig. 5A and B). In the NMR experimental structure, position E160 of IFN-α2 appears to have a mobile side chain that switches H-bond partners from IFN-α2 S11 and T156 to IFN-α2 R12 and/or IFNAR-2 H76. The replacement of E160 with the

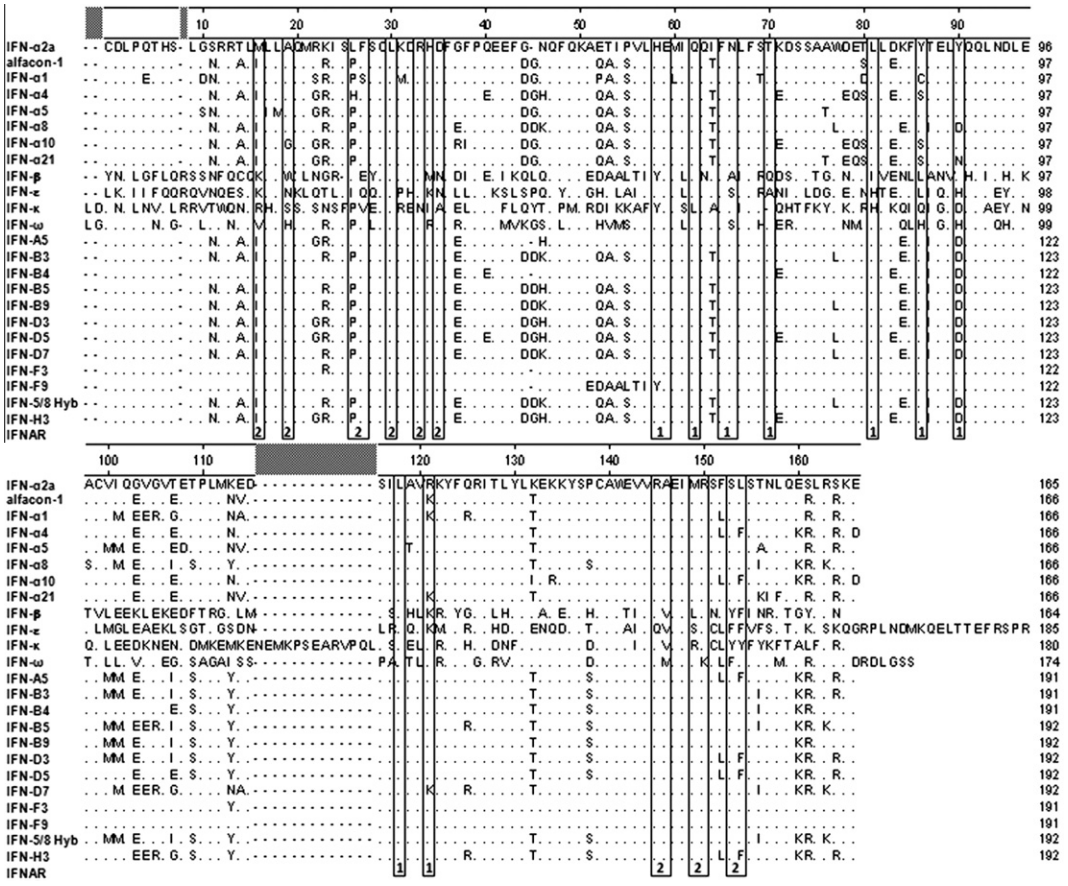

Fig. 4. Sequence comparison of the final set of 12 hybrid IFNs to the type I IFN parents and alfacon-1. Gene sequences were determined for each of the hybrid IFNs, and derived amino acid sequences were aligned using the Clustal W method with Lasergene MegAlign (DNASTAR, Madison, WI). Numbering is according to that of IFN-alfacon-1. Amino acids identical to IFN-α2a are hidden. Residues previously shown to be important for receptor binding to IFNAR-1 or IFNAR-2 are indicated by 1 or 2, respectively, beneath the boxed amino acids (Piehler and Schreiber, 1999; Slutzki et al., 2006; Uze et al., 2007). The N-terminal extensin secretory signal peptide and the C-terminal 6x-His-KDEL sequence tags which were present on each of the hybrid IFNs are not shown in this alignment.

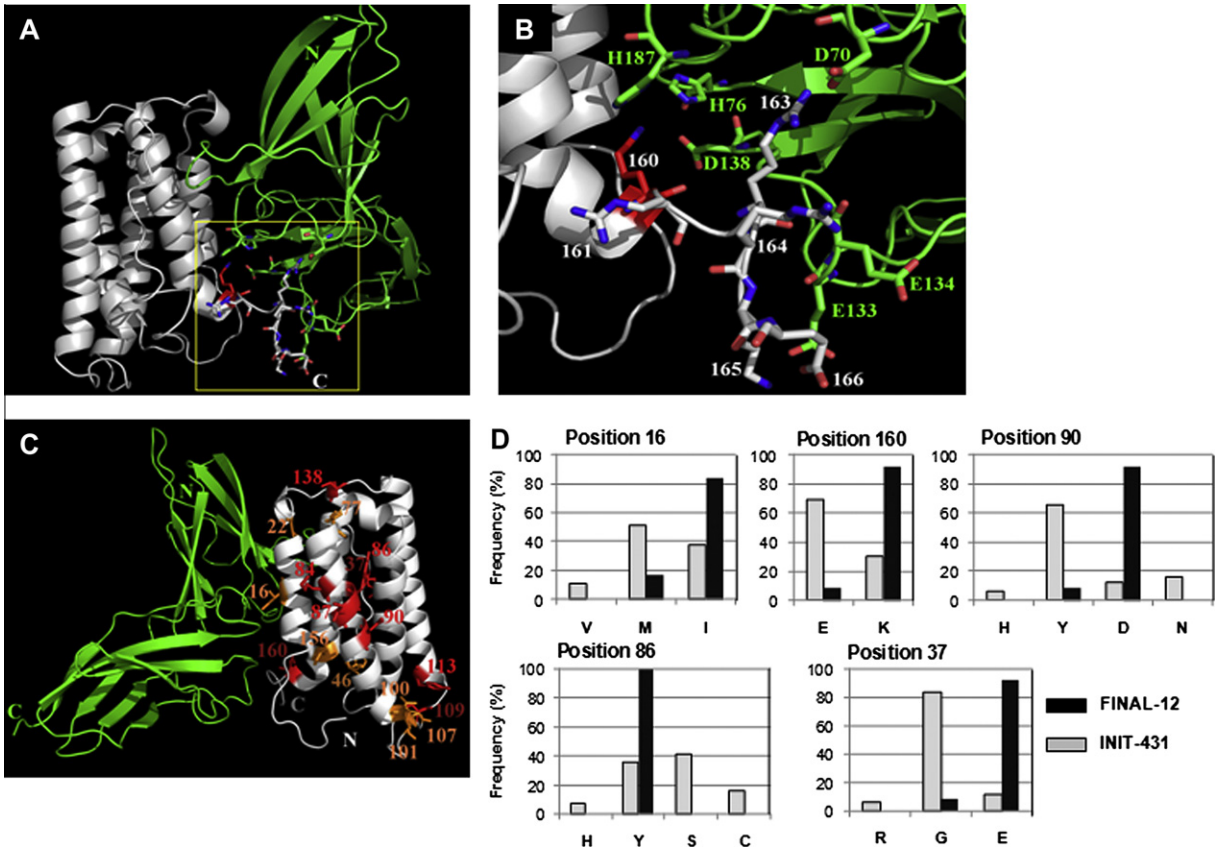

Fig. 5. Structural modeling of potential influences on binding of hybrid IFNs to IFNAR-2. (A) A ribbon diagram constructed for a representative hybrid IFN, (IFN-H3, white) is shown bound to IFNAR-2 (green) with the C-terminal tail boxed (yellow). (B) The boxed region shown is enlarged to show predicted residue-residue interactions involving the C-terminal tail (positions 160–166). (C) A ribbon diagram of hybrid IFN-H3 (white) complexed with IFNAR-2 (green) shows amino acids demonstrating strong selective pressure with red indicating a >50% change in frequency and orange a 30–50% change in frequency. Predicted side chain locations are indicated. (D) The amino acid frequency (%) at amino acid positions 16, 160, 90, 86, and 37 (with numbers corresponding to those in Fig. 4) observed among an initial pool of 431 hybridized IFNs (INIT-431) resulting from early rounds of GRAMMR and those of the final set of 12 hybrid IFNs (FINAL-12) are depicted.

positively-charged K160 residue in most of the hybrid IFNs (e.g. IFN-H3, Fig. 5B) would have a marked effect on the dynamics of the neighboring residues. R161, which is present in all of the charged tails of the hybrid IFNs, is predicted to interact with one or two negatively-charged residues within the same IFN molecule: a D residue common at position 44 and/or E40. When position 161 is occupied by S (as in IFN-α2a and the hybrid IFNs with a 0 charge tail), none of these negative residues are present in that same IFN molecule.

To identify selection pressures within the hybrid genes, we performed a frequency comparison of individual amino acids at each position among the FINAL-12 IFNs and 431 other hybrid IFNs (INIT-431) from early rounds of GRAMMR. The most highly selected residues were mapped onto the IFN-H3 model (Fig. 5C). Clear biases were observed both toward selection of specific amino acids implicated in receptor binding (e.g. positions 16 and 160 for IFNAR-2 and position 90 for IFNAR-1) as well as toward amino acids not known to relate to IFNAR binding (e.g. position 37, Fig. 5D). In some cases, almost all of the FINAL-12 had an amino acid at a certain position that was not the most prevalent one among INIT-431 (e.g., position 37, Fig. 5D). A more complete listing of favored residues identified is presented in Supplemental Table 4.

Structural models were also used to correlate increased antiviral activities of the hybrid IFNs by comparison to parental genes. We aligned the predicted amino acid sequences of the hybrid IFNs to determine the minimum number of parents required to produce each hybrid sequence. By mapping the residue differences between parents into structural models, we identified several potential interactions that could contribute to increased antiviral activity, some of which support the importance of interaction between more positively charged tails and IFNAR-2. For example, IFN-B3 differs by only two residues from IFN-5/8 Hyb, so the higher IC_{50} and IC_{90} values measured for the IFN-B3 molecule (Supplemental Table 2) likely relate to the two R residues at the C-terminal end of the molecule that were inherited from IFN-α4. The structural model of IFN-B3 predicts that both of these residues interact directly with IFNAR-2, probably leading to increased binding (Fig. 6, A and B). An equivalent analysis for IFN-B9 leads to a similar conclusion (Fig. 6C).

In contrast, the increased antiviral activity of some of the IFNs cannot be attributed to IFN–IFNAR-2 interactions. As mentioned already, IFN-F9 is essentially IFN-α2a with residues 51–58 from IFN-β. When mapped into a three-dimensional model, this fragment appears as part of an α-helix that lies on the opposite side of the interaction of the IFN with IFNAR-2 (Fig. 6D). This area includes amino acids shown through earlier mutational analysis to be important for IFNAR-1 binding (Roisman et al., 2005). Likewise, the increased antiviral activity of IFN-D7 cannot be explained by a direct alteration of the known IFN-IFNAR-2 interaction surface, but it is possible that the observed changes impact interactions with IFNAR-1 (Fig. 5E). Similar analyses of the remaining hybrid IFN sequences showed that residue optimization tended to occur in different regions on the IFN molecules, distant from the experimentally observed IFN–IFNAR-2 interaction surface and not in regions known for binding to IFNAR-1 (e.g., IFN-D5, Fig. 5F).

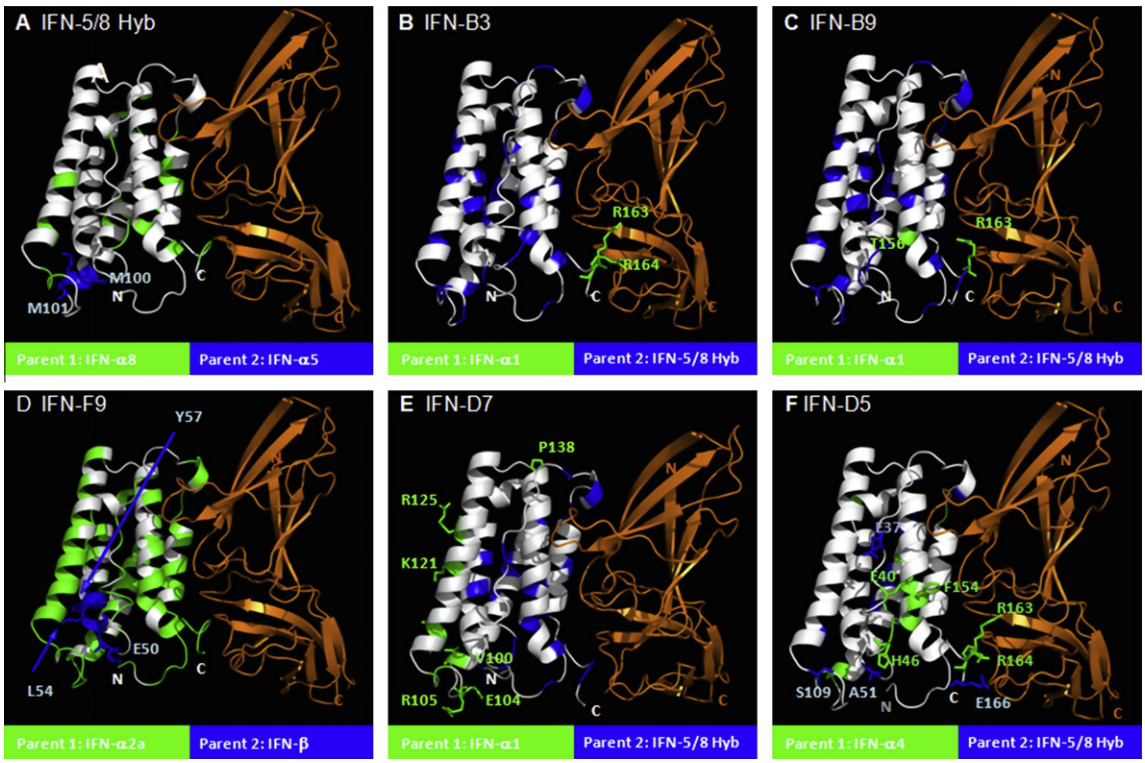

Fig. 6. Structural modeling of selected hybrid IFNs: showing relationship between potency and residue inheritance. (A–F) Ribbon models are shown for selected hybrid IFNs bound to IFNAR-2 (orange) showing the inferred parental sequences in green or blue. Residues identical in both parents are shown in white. Residues identified as being important for potency are shown with side residues in the predicted orientation.

4. Discussion

This study had two major goals: (1) to derive synthetic human IFNs with increased antiviral activities as compared to natural IFNs against a broad range of highly pathogenic viruses; and, (2) to gain a basic understanding of the factors that contributed to improved IFN potency. We created the novel IFNs using GRAMMR, a unique, non-PCR based method that can blend sizeable and diverse genes producing mostly functional hybrid genes. This method favors recovery of the hybrid genes over re-annealed homologous parent strands because homoduplex DNAs remain linear whereas heteroduplex DNAs circularize due to staggered termini created during linearization and because circular DNA can transform bacteria more efficiently than linear DNA. Our expression approach, introducing infectious RNA into *N. benthamiana* plants, was easy to use to produce thousands of hybrid IFNs in small quantities and has the capacity to generate protein quantities in excess of 1 g of recombinant protein/kg of plant tissue. Plants offer additional advantages such as enzymes that can facilitate proper conformations of mammalian-derived proteins and the absence of harmful proteins such as endotoxins, which occur in bacteria, or oncogenic viruses sometimes found in mammalian cells. A similar system used to produce therapeutic proteins has been shown safe in clinical studies (McCormick et al., 2008) and was used to generate large quantities of an entry inhibitor for HIV-1 (O'Keefe et al., 2009). Therefore, plant-derived IFNs could serve as a safe and effective alternative to currently used bacterial production methods.

To address our aim of identifying IFNs with enhanced broad-spectrum potency, we compared the antiviral activities of more than 1400 plant-derived, hybrid IFNs against three RNA viruses and one DNA virus from four different families: *Filoviridae* (EBOV), *Bunyaviridae* (RVFV), *Togaviridae* (VEEV), and *Poxviridae* (MPXV). Evolutionary pressures applied in our development process included both primary selection for high expression levels in plants and secondary selection for strong antiviral activity against these four dissimilar, highly pathogenic viruses with varying sensitivities to type I IFN. In particular, the DNA virus, MPXV, was not expected to be as susceptible to the antiviral properties of the IFNs as the RNA viruses, yet we did see improved activity against MPXV with numerous hybrid IFNs. Our final set showed enhanced activity against all of the viruses *in vitro* as compared to IFN-α2a. While we did not do extensive comparisons of the final set of 12 hybrid IFNs to pharmaceutical grade IFN-alfacon-1 (Infergen), we did compare them in early screenings both to Infergen and to plant-derived IFN-alfacon-His. Of note, we detected many hybrid IFNs that performed as well as or better than the consensus IFNs against one or more of the viruses. Moreover, despite being a less refined preparation, we found that the plant-derived IFN-alfacon-1-His was almost as effective against the tested viruses as Infergen; thus, in addition to producing novel IFNs, the plant expression system could offer a more convenient and cost-effective means to manufacture large quantities of IFN-alfacon than methods currently in use.

To gain an understanding of factors that might have contributed to the potency of our hybrid IFNs, we compared their nucleotide sequences to those of the parents. We noted numerous, consistently selected amino acids at cognate locations of the hybrid IFNs. Many of these changes are also present in IFN-alfacon-1, which is more potent than the natural type I IFNs. The increased potency of IFN-alfacon-1 has been attributed to a greater receptor binding affinity (Blatt et al., 1996; Klein et al., 1996), engagement of increased numbers of both high and low affinity receptors (Klein et al., 1996), and increased expression of certain IFN response genes (Klein et al., 1993). We suspect that some of the changes that we noted relate to the enhanced antiviral activity of IFN-alfacon-1 as well as our hybrid IFNs.

With respect to receptor binding, we observed unique positively charged C-terminal tails among our hybrid IFNs which, when mapped into a three-dimensional model of IFN–IFNAR-2, supports earlier data showing that replacing the C-terminal tail of IFN-α2 with the more positively charged tail of IFN-α8 (which included the same K160 and R161 residues as seen in our hybrid IFNs) increases the IFN's affinity for IFNAR-2 and is likely responsible for enhanced potency (Slutzki et al., 2006). Additional amino acid changes in the hybrid IFNs were also predicted to impact binding to IFNAR-2 as deduced from their proximity to the binding faces of the proteins when they were mapped to a recently solved experimental structure of IFN-α2 complexed with IFNAR-2, but others were located quite far from the interacting surfaces of the proteins. Based on earlier mapping studies, we can surmise that some of these are related to IFNAR-1 binding, but confirmation of this hypothesis would require an experimental structure showing IFN–IFNAR-1 binding.

In summary, this study demonstrates that it is possible to generate novel IFNs with enhanced *in vitro* activity against multiple highly pathogenic viruses and that the improvement is due at least in part to changes that are expected to influence receptor binding. Our work also indicates that plant-derived IFNs can be as potent as the homologous, commercially available, bacterial-derived IFN *in vitro*. Additional studies will be required to validate these findings *in vivo*.

Acknowledgements

We acknowledge Dr. Jason Paragas and Dr. Steven Fong for helping to establish this project. JWK and BFB were supported by National Research Council Postdoctoral Research Associateships. This research was supported in part by the Defense Threat Reduction Agency (DTRA) and the U.S. Department of Defense High Performance Computing Modernization Program (HPCMP) under the High Performance Computing Software Applications Institutes (HSAI) initiative. This research was performed under a U.S. Army Medical Research and Material Command Cooperative Research and Development Agreement between USAMRIID and Novici Biotech, LLC. The opinions, interpretations, conclusions, and recommendations contained herein are those of the authors and are not necessarily endorsed by the U.S. Army.

Appendix A. Supplementary data

Supplementary data associated with this article can be found, in the online version, at doi:10.1016/j.antiviral.2011.10.008.

References

Beitzel, B.F., Bakken, R.R., Smith, J.M., Schmaljohn, C.S., 2010. High-resolution functional mapping of the venezuelan equine encephalitis virus genome by insertional mutagenesis and massively parallel sequencing. PLoS Pathog. 6, e1001146.

Berman, H.M., Westbrook, J., Feng, Z., Gilliland, G., Bhat, T.N., Weissig, H., Shindyalov, I.N., Bourne, P.E., 2000. The protein data bank. Nucleic Acids Res. 28, 235–242.

Blatt, L.M., Davis, J.M., Klein, S.B., Taylor, M.W., 1996. The biologic activity and molecular characterization of a novel synthetic interferon-alpha species, consensus interferon. J. Interferon Cytokine Res. 16, 489–499.

Bouloy, M., Janzen, C., Vialat, P., Khun, H., Pavlovic, J., Huerre, M., Haller, O., 2001. Genetic evidence for an interferon-antagonistic function of rift valley fever virus nonstructural protein NSs. J. Virol. 75, 1371–1377.

Carreno, V., Porres, J.C., Mora, I., Bartolome, J., Bas, C., Gutiez, J., Cortes, J., Hernandez Guio, C., 1987. Prolonged (6 months) treatment of chronic hepatitis B virus infection with recombinant leukocyte A interferon. Liver 7, 325–332.

De Loose, M., Gheysen, G., Tire, C., Gielen, J., Villarroel, R., Genetello, C., Van Montagu, M., Depicker, A., Inze, D., 1991. The extensin signal peptide allows secretion of a heterologous protein from protoplasts. Gene 99, 95–100.

Fernandez de Marco Mdel, M., Alejo, A., Hudson, P., Damon, I.K., Alcami, A., 2009. The highly virulent variola and monkeypox viruses express secreted inhibitors of type I interferon. FASEB J. 24, 1479–1488.

Fried, M.W., Shiffman, M.L., Reddy, K.R., Smith, C., Marinos, G., Goncales Jr., F.L., Haussinger, D., Diago, M., Carosi, G., Dhumeaux, D., Craxi, A., Lin, A., Hoffman, J., Yu, J., 2002. Peginterferon alfa-2a plus ribavirin for chronic hepatitis C virus infection. N. Engl. J. Med. 347, 975–982.

Geisbert, T.W., Lee, A.C., Robbins, M., Geisbert, J.B., Honko, A.N., Sood, V., Johnson, J.C., de Jong, S., Tavakoli, I., Judge, A., Hensley, L.E., Maclachlan, I., 2010. Postexposure protection of non-human primates against a lethal Ebola virus challenge with RNA interference. A proof-of-concept study. Lancet 375, 1896–1905.

Giritch, A., Marillonnet, S., Engler, C., van Eldik, G., Botterman, J., Klimyuk, V., Gleba, Y., 2006. Rapid high-yield expression of full-size IgG antibodies in plants coinfected with noncompeting viral vectors. Proc. Natl. Acad. Sci. USA 103, 14701–14706.

Glue, P., Fang, J.W., Rouzier-Panis, R., Raffanel, C., Sabo, R., Gupta, S.K., Salfi, M., Jacobs, S., 2000. Pegylated interferon-alpha2b: pharmacokinetics, pharmacodynamics, safety, and preliminary efficacy data. Hepatitis C Intervention Therapy Group. Clin. Pharmacol. Ther. 68, 556–567.

Goff, A., Mucker, E., Raymond, J., Fisher, R., Bray, M., Hensley, L., Paragas, J., 2011. Infection of cynomolgus macaques with a recombinant monkeypox virus encoding green fluorescent protein. Arch. Virol. 156, 1877–1881.

Ikegami, T., Won, S., Peters, C.J., Makino, S., 2006. Rescue of infectious rift valley fever virus entirely from cDNA, analysis of virus lacking the NSs gene, and expression of a foreign gene. J. Virol. 80, 2933–2940.

Jahrling, P.B., Hesse, R.A., Eddy, G.A., Johnson, K.M., Callis, R.T., Stephen, E.L., 1980. Lassa virus infection of rhesus monkeys: pathogenesis and treatment with ribavirin. J. Infect. Dis. 141, 580–589.

Klaus, W., Gsell, B., Labhardt, A.M., Wipf, B., Senn, H., 1997. The three-dimensional high resolution structure of human interferon alpha-2a determined by heteronuclear NMR spectroscopy in solution. J. Mol. Biol. 274, 661–675.

Klein, S.B., Blatt, L.M., Taylor, M.W., 1993. Consensus interferon induces peak mRNA accumulation at lower concentrations than interferon-alpha 2a. J. Interferon Res. 13, 341–347.

Klein, S.B., Blatt, L.M., Taylor, M.W., 1996. Cell surface binding characteristics correlate with consensus type I interferon enhanced activity. J. Interferon Cytokine Res. 16, 1–6.

Lee, M.S., Bondugula, R., Desai, V., Zavaljevski, N., Yeh, I.C., Wallqvist, A., Reifman, J., 2009. PSPP: a protein structure prediction pipeline for computing clusters. PLoS ONE 4, e6254.

Ma, J.K., Drake, P.M., Christou, P., 2003. The production of recombinant pharmaceutical proteins in plants. Nat. Rev. Genet. 4, 794–805.

Mateo, M., Reid, S.P., Leung, L.W., Basler, C.F., Volchkov, V.E., 2010. Ebolavirus VP24 binding to karyopherins is required for inhibition of interferon signaling. J. Virol. 84, 1169–1175.

McCormick, A.A., Reddy, S., Reinl, S.J., Cameron, T.I., Czerwinkski, D.K., Vojdani, F., Hanley, K.M., Garger, S.J., White, E.L., Novak, J., Barrett, J., Holtz, R.B., Tuse, D., Levy, R., 2008. Plant-produced idiotype vaccines for the treatment of non-Hodgkin's lymphoma: safety and immunogenicity in a phase I clinical study. Proc. Natl Acad. Sci. USA 105, 10131–10136.

Munro, S., Pelham, H.R., 1987. A C-terminal signal prevents secretion of luminal ER proteins. Cell 48, 899–907.

Nederman, T., Karlstrom, E., Sjodin, L., 1990. An in vitro bioassay for quantitation of human interferons by measurements of antiproliferative activity on a continuous human lymphoma cell line. Biologicals 18, 29–34.

Nudelman, I., Akabayov, S.R., Schnur, E., Biron, Z., Levy, R., Xu, Y., Yang, D., Anglister, J., 2010. Intermolecular interactions in a 44 kDa interferon-receptor complex detected by asymmetric reverse-protonation and two-dimensional NOESY. Biochemistry 49, 5117–5133.

O'Keefe, B.R., Vojdani, F., Buffa, V., Shattock, R.J., Montefiori, D.C., Bakke, J., Mirsalis, J., d'Andrea, A.L., Hume, S.D., Bratcher, B., Saucedo, C.J., McMahon, J.B., Pogue, G.P., Palmer, K.E., 2009. Scaleable manufacture of HIV-1 entry inhibitor griffithsin and validation of its safety and efficacy as a topical microbicide component. Proc. Natl Acad. Sci. USA 106, 6099–6104.

Ozes, O.N., Reiter, Z., Klein, S., Blatt, L.M., Taylor, M.W., 1992. A comparison of interferon-Con1 with natural recombinant interferons-alpha: antiviral, antiproliferative, and natural killer-inducing activities. J. Interferon Res. 12, 55–59.

Palacios, G., Quan, P.L., Jabado, O.J., Conlan, S., Hirschberg, D.L., Liu, Y., Zhai, J., Renwick, N., Hui, J., Hegyi, H., Grolla, A., Strong, J.E., Towner, J.S., Geisbert, T.W., Jahrling, P.B., Buchen-Osmond, C., Ellerbrok, H., Sanchez-Seco, M.P., Lussier, Y., Formenty, P., Nichol, M.S., Feldmann, H., Briese, T., Lipkin, W.I., 2007. Panmicrobial oligonucleotide array for diagnosis of infectious diseases. Emerg. Infect. Dis. 13, 73–81.

Petrey, D., Xiang, Z., Tang, C.L., Xie, L., Gimpelev, M., Mitros, T., Soto, C.S., Goldsmith-Fischman, S., Kernytsky, A., Schlessinger, A., Koh, I.Y., Alexov, E., Honig, B., 2003. Using multiple structure alignments, fast model building, and energetic analysis in fold recognition and homology modeling. Proteins 53 (Suppl. 6), 430–435.

Piehler, J., Schreiber, G., 1999. Mutational and structural analysis of the binding interface between type I interferons and their receptor Ifnar2. J. Mol. Biol. 294, 223–237.

Platanias, L.C., 2005. Mechanisms of type-I- and type-II-interferon-mediated signalling. Nat. Rev. Immunol. 5, 375–386.

Rider, T.H., Zook, C.E., Boettcher, T.L., Wick, S.T., Pancoast, J.S., Zusman, B.D., 2011. Broad-spectrum antiviral therapeutics. PLoS ONE 6, e22572.

Roisman, L.C., Jaitin, D.A., Baker, D.P., Schreiber, G., 2005. Mutational analysis of the IFNAR1 binding site on IFNalpha2 reveals the architecture of a weak ligand-receptor binding-site. J. Mol. Biol. 353, 271–281.

Samuel, C.E., 2001. Antiviral actions of interferons. Clin. Microbiol. Rev. 14, 778–809 (table of contents).
Simmons, J.D., White, L.J., Morrison, T.E., Montgomery, S.A., Whitmore, A.C., Johnston, R.E., Heise, M.T., 2009. Venezuelan equine encephalitis virus disrupts STAT1 signaling by distinct mechanisms independent of host shutoff. J. Virol. 83, 10571–10581.
Slutzki, M., Jaitin, D.A., Yehezkel, T.B., Schreiber, G., 2006. Variations in the unstructured C-terminal tail of interferons contribute to differential receptor binding and biological activity. J. Mol. Biol. 360, 1019–1030.
Uze, G., Schreiber, G., Piehler, J., Pellegrini, S., 2007. The receptor of the type I interferon family. Curr. Top. Microbiol. Immunol. 316, 71–95.
Weaver, J.R., Isaacs, S.N., 2008. Monkeypox virus and insights into its immunomodulatory proteins. Immunol. Rev. 225, 96–113.
Yin, J., Gardner, C.L., Burke, C.W., Ryman, K.D., Klimstra, W.B., 2009. Similarities and differences in antagonism of neuron alpha/beta interferon responses by Venezuelan equine encephalitis and Sindbis alphaviruses. J. Virol. 83, 10036–10047.